Investigation of the impact of liquid presence on the acoustic streaming generated by a vibrating sharp tip capillary

Chong Li, Balapuwaduge Lihini Mendis, Lisa Holland, Peng Li*

C. Eugene Bennett Department of Chemistry, West Virginia University, Morgantown, WV 26506, USA.

* Corresponding author: peng.li@mail.wvu.edu

Abstract

Sharp edge structures have been demonstrated as an efficient way of generating acoustic streaming in microfluidic devices, which finds numerous applications in fluid mixing, pumping, particle actuation, and cell lysis. A sharp tip capillary is widely available means of generating sharp structures without the need of microfabrication, which has been used for studying enzyme kinetics, droplet digital PCR, and mass spectrometry analysis. In this work, we studied the influence of liquid inside the vibrating glass capillary on its efficiency of generating acoustic streaming. Using fluorescence microscopy and fluorescent particles, we observed that adding liquid to the inside of the vibrating glass capillary changed the streaming patterns as well as led to increased streaming velocity. Based on the observed streaming patterns, we hypothesized the liquid present in the capillary changed vibration mode of the capillary, which is matched with COMSOL simulations. Finally, the utility of the liquid filled vibrating capillary was demonstrated for higher energy efficiency for fluid mixing and mass spectrometry experiments. This study will provide useful guidance when optimizing the efficiency of vibrating sharp tip capillary systems.

Keywords: Acoustic streaming, Vibrating Capillary, Acoustic Mixing, Acoustic Droplet Generation,

Statements and Declarations

Competing Interests: L.H. and P.L. has filed a provisional patent application on the vibrating capillary based capillary electrophoresis mass spectrometry system.

Introduction

Acoustic streaming is a time-averaged steady flow caused by the dissipation of acoustic energy in the fluid.(Mitome 1998) In recent years, it has become an increasingly important tool for manipulating fluids and particles at microscale.(Bruus et al. 2011) Depending on the position where the acoustic energy attenuation mainly occurs, the acoustic streaming can be classified into two types: Eckart streaming (quartz wind) and Rayleigh-Schlichting streaming (boundary layer driven streaming).(Zhang et al. 2020) In Eckart streaming, as the distance from the acoustic source increases, the amplitude of the acoustic wave attenuates, and the acoustic pressure amplitude will decrease. The dissipation of acoustic energy results in a transfer of momentum to the flow, generating the acoustic streaming along the direction of acoustic propagation. (Tang et al. 2017, Kolesnik et al. 2021) Rayleigh-Schlichting streaming formed by the viscous dissipation of acoustic energy into the viscous boundary layer (VBL) of a fluid along any solid boundary that is comparable or greater in length than a quarter of the acoustic wavelength. At low enough frequency, the acoustic energy dissipation into the viscous boundary layer (VBL) is larger in comparison to bulk dissipation, therefore, a strong velocity gradient is formed perpendicular to the solid boundary as the acoustic wave propagates parallel to it. The strong velocity gradient will create vortices in viscous boundary layers between solid wall and fluid. Rayleigh-Schlichting streaming has a close relationship with boundary layer, it can be formed around various geometry walls in fluid with acoustic vibration field, resulting in various configurations of streaming flow under different conditions. (Zhang 2020, Zhang, Guo et al. 2020, Lin et al. 2021) At the microscale, by creating different boundary structures, boundary driven acoustic streaming has been demonstrated to achieve many fluids and particle manipulation functionalities including fluid pumping, (Du et al. 2009, Patel et al. 2014) mixing, (Ahmed et al. 2009, Luong et al. 2010, Cardoso et al. 2014) gradient generation, (Destgeer, Im et al. 2014, Liang et al. 2020) particle trapping/separation, (Jalal and Leong 2018, Charrier-Mojtabi et al. 2019, Li et al. 2021) and cell lysis.(Yeo and Friend 2009, Wang et al. 2019) Particularly, recent works on generating acoustic streaming with sharp-edge structures have greatly improved the efficiency and flexibility of acoustic streaming devices, (Huang et al. 2013, Huang et al. 2014, Huang et al. 2018, Li et al. 2019, Durrer et al. 2022, Pavlic et al. 2023) allowing simple and miniaturized driving systems (e.g. Arduino based driving circuit).(Bachman et al. 2018) In addition to microfabricated structures, acoustic streaming can also be generated by vibrating solid objects emersed in fluids. Peerhossaini et al. have demonstrated vibration induced streaming around a metal beam in water/glycerin solution.(Costalonga et al. 2016) Garimella and co-workers studied twodimensional streaming flows induced by resonating thin beams, and experimental results were in close agreement with the predicted streaming flows.(Acıkalın et al. 2003) The research from Hu's group revealed that in needle–liquid–substrate system, the ultrasonic needle's vibration can generate the acoustic streaming field capable of concentrating micro-/nanoscale materials.(Tang et al. 2018)

Recently, our group reported that a vibrating pulled glass capillary can also generate acoustic streaming with high efficiency. This method has been used to generate droplets for MS analysis, (Ranganathan et al. 2019, Li et al. 2020, DeBastiani et al. 2021, Majuta et al. 2021) as a portable droplet generation system for ultra-wide dynamic range digital polymerase chain reaction (PCR)(He et al. 2021) and as a mixer for one-step enzyme kinetics measurement.(Li et al. 2021) Despite of the diverse applications demonstrated, understanding of the impact of various experimental factors is still limited. To further improve the performance of vibrating pulled glass capillary and the capillary vibrating sharp-edge spray ionization (cVSSI) device, it is important to study the potential factors that can affect the streaming patterns that induced by a vibrating sharpedge glass capillary. Although existing works studied the impact of relative position of substrate, (Tang, Liu et al. 2018) the viscosity, boundary layer thickness, geometry etc. (Zhang, Guo et al. 2020) for microfabricated PDMS sharp edge structures, the setup of a vibrating capillary introduces some unique factors, which has not been studied before. One of the notable factors is the presence of liquid in the capillary. For many applications such as micro-mixing, and capillary electrophoresis-vibrating sharp-edge spray ionization-mass spectrometry (CE-VSSI-MS), (Kristoff et al. 2020) it is possible to employ either the absence of liquid in capillary or presence of liquid in the capillary setup. Therefore, it is of great importance to elucidate the impact of liquid inside the vibrating sharp-edge glass capillary on the device performance. This work studies the impact of liquid inside the vibrating glass capillary on its streaming patterns. Results show that the liquid inside the glass capillary can change the streaming patterns of vibrating glass capillary as well as the streaming velocity. The COMSOL simulation for streaming patterns matches well with the experimentally observed streaming patterns for both the liquid-filled capillary and air-filled capillary. With the higher streaming velocity generated by a liquid-filled capillary, the high performance is demonstrated for fluid mixing and droplets generation. This study will provide guidance when optimizing the working efficiency for VSSI devices, and liquid-filling is an importance factor that needs to be taken into consideration for the vibrating glass capillary in the future.

Methods and materials

Reagents and material

LC/MS water and potassium permanganate (KMnO₄) were purchased from Sigma-Aldrich; Formic acid (HCOOH) was purchased from Fischer Chemical; Octadecyltrichlorosilane (OTS), toluene and clarithromycin ($C_{38}H_{69}NO_{13}$, *m.w.* 747.96) were purchased from TCI chemical. 1x phosphate-buffered saline (PBS) solution was bought from VWR life science. These chemicals were directly used without further purification.10 µm beads solution (Fluoresbrite Plain YG, CV = 10%) was bought from Polysciences Inc. (PA). The 10 µm beads solution was diluted to 10^{-5} of its original concentration with 1x PBS solution before the tests. 1.2 mg/mL KMnO₄ in water was used for the mixing test. The 20 µm (TP20W1) capillaries were bought from WPI company.

Device fabrication

The fabrication of vibrating glass capillary device was similar with previous reports.(Ranganathan et al. 2019) The glass capillary (TP20W1) capillary was purchased from WPI inc. The vibrating glass capillary device was made by attaching a piezoelectric transducer (7BB-27-4 L0, Murata) to one piece of clean No. 1 cover glass (24 mm X 60 mm, VWR) using epoxy glue (5 min epoxy, Devcon). Then the 20 µm ID (TP20W1) glass capillary was attached to the cover glass with glass glue (Loctite Glass Glue Crystal Clear). The glass capillary has an OD of ~36 µm (Figure S1). The angle between the cover glass bottom edge and capillary was 60 degrees (Figure 1a). After the glass glue was dried, the device was ready to use. To generate the mechanical vibration, a function waveform generator (RIGOL DG4102), a power amplifier (Krohn-Hite 7500) and piezoelectric transducer of the vibrating capillary device were connected to generate the vibration. The working frequency and amplitude of the capillary VSSI device can be tuned by the function waveform generator.

Streaming experiment setup

To prepare the air-filled capillary, the end of the 20 µm glass capillary was first dipped into 10 mM OTS in toluene solution. Then the 20 µm glass capillary was placed at room temperature for 30 min, and the excess OTS solution inside the capillary was removed by the airflow from a microfiller. The glass capillary was kept in oven under 75 °C for 12 h. The purpose of OTS coating is to create a hydrophobic inner wall surface so that the liquid cannot go inside. The OTS coated glass capillary was used for liquid absent (air-filled capillary) streaming experiment. After the streaming experiment was done with liquid absent glass capillary, the capillary was filled with 1x PBS solution as the liquid presence (liquid-filled capillary) condition to test the streaming.

To observe the streaming patterns, the glass capillary was inserted into a cubic plastic reservoir

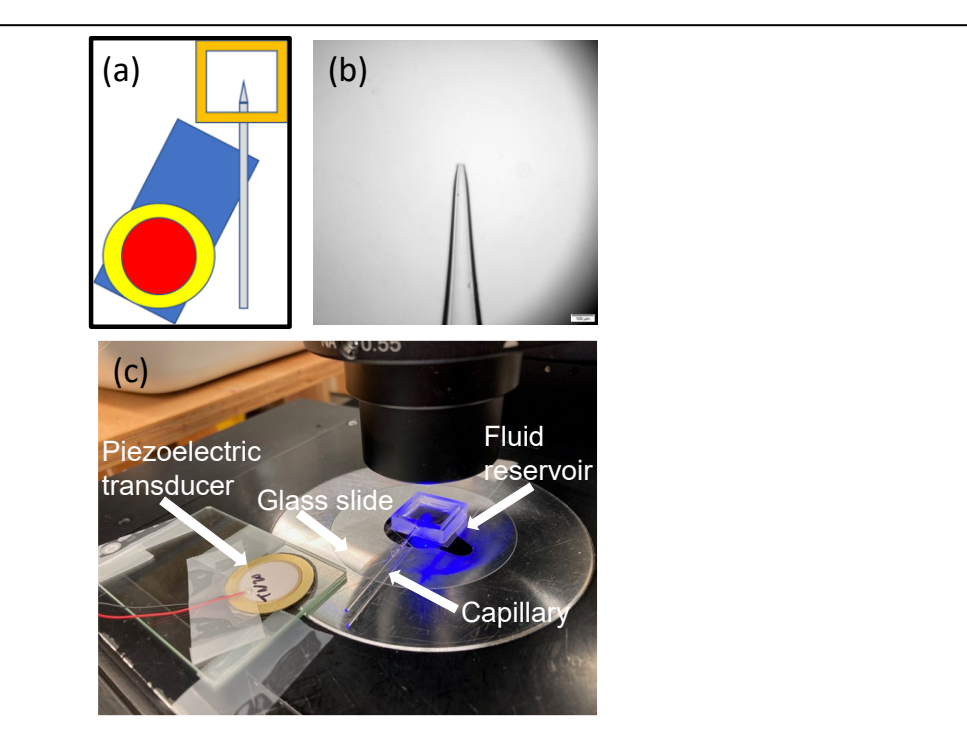


Figure 1. Streaming patterns experiment set-up. (a) Schematic of the streaming experiment set-up. (b) 20 μ m glass capillary. Scale bar represents 100 μ m. (c) Streaming experiment set-up under the Olympus IX73 microscope.

(20 mm x 20 mm x 5 mm) through a small hole (3 mm I.D.) at one side of the reservoir. The surface of the small hole was coated with OTS so that the reservoir did not have any leakage during the streaming experiment. The reservoir was filled with 1 mL 10 μ m beads solution and the glass capillary was immersed into the bead solution. The glass capillary end was placed at the center of this cubic reservoir (Figure 1a and 1b). The streaming pattern was monitored and recorded using an Olympus IX 73 microscope with 4 x objective lens. The measurement window is ~0.7-1 mm above the capillary tip (Figure S2). The bottom of the reservoir is a piece of transparent glass slide, and the fluorescence can pass through to illuminate the 10 μ m beads (Figure 1c). The exposure time of streaming video was 10 ms. The obtained video files were process by the ImageJ software for analysis.

Acoustic streaming velocity measurements

To measure the streaming velocity, we collect the video files for the beads streaming patterns under different input voltages. The collected video files were exported to TIFF sequences with the Olympus CellSense software. Through the ImageJ software, the TIFF files were converted to an image sequence so that the beads movement can be tracked. The time interval between two

adjacent frames is obtained from the sCMOS camera. Through measuring the bead moving distance between two adjacent frames, we can calculate the velocity of selected beads.

COMSOL modeling of acoustic streaming

In the present study, the perturbation theory was employed for computing the acoustic streaming pattern, which provides a convenient means of studying streaming patterns generated by a vibrating capillary. (Nyborg 1958) By neglecting the non-linear term, the first order field can be solved based on the linearized Navier-Stokes equation. Although it has been pointed out that the perturbation theory method tends to overestimate the streaming velocity at high vibration velocities, the present work focused on the qualitative evaluation of streamlining patterns and maintained streaming velocities <40 mm/s, which has shown good agreement with experimental results for vibrating sharp-edges. (Ovchinnikov et al. 2014) Briefly, the Navier-Stokes equation (eqn 1) and the continuity equation (eqn 2) can be decomposed into two parts: a first order oscillating field (\mathbf{v}_1) and a second order dynamic field (\mathbf{v}_2) involving a steady component (eqn 3a and 3b). Here, the liquid is considered incompressible given the low Mach number in the present system (Zhang et al. 2020).

$$\frac{\partial \mathbf{v}}{\partial t} + (\mathbf{v} \cdot \nabla)\mathbf{v} = -\frac{1}{\rho}\nabla p + \upsilon \nabla^2 \mathbf{v}$$
 (1)

$$\nabla \cdot \mathbf{v} = 0 \tag{2}$$

$$p = p_1 + p_2 \tag{3a}$$

$$\mathbf{v} = \mathbf{v}_1 + \mathbf{v}_2 \tag{3b}$$

 p_1 and p_2 are the first and second order acoustic pressure field, respectively. ρ is the density of fluid, and v is the kinematic viscosity of the fluid. The first order field can be described as:

$$\frac{\partial \mathbf{v_1}}{\partial t} + (\mathbf{v} \cdot \nabla)\mathbf{v} = -\frac{1}{o}\nabla p_1 + \upsilon \nabla^2 \mathbf{v_1}$$
 (4)

Here, neglecting the nonlinear term $(\mathbf{v} \cdot \nabla)\mathbf{v}$ gives the linearized Navier-Stokes equation for solving the first order velocity field. The second order steady state field can be obtained by substituting Eqns 3a and 3b to Eqn 1 and 2 performing time average:

$$(\mathbf{v}_2 \cdot \nabla)\mathbf{v}_2 + \langle (\mathbf{v}_1 \cdot \nabla)\mathbf{v}_1 \rangle = -\frac{1}{\rho} \nabla p_2 + \nu \nabla^2 \mathbf{v}_2$$
 (5)

Acoustic streaming field is thus obtained by solving for $\mathbf{v_2}$. $\langle \cdots \rangle$ denotes the time average operation over one vibration period, which is time independent. Eqn (5) can be solved after solving the acoustic velocity ($\mathbf{v_1}$) and pressure of the first order field.

Here, we used the finite element method software COMSOL Multiphysics® (version 6.0) to perform the numerical simulation. Here we chose to simulate 2D geometry because when we observed the streaming pattern induced by a vibrating capillary, we observed that the dominant streaming pattern existed only in one layer. While beads movement can be seen in other layers, they are much weaker compared with the observed layer. In this work, since we focused on the dominant pattern, the 2D model allows us to evaluate the streaming pattern with low cost. For future studies, it will be worth to investigate the streaming patter in 3D using efficient 3D modeling strategies. (Pavlic, Roth et al. 2023) The simulated domain consists of a 4*4 mm liquid domain and a capillary domain. The liquid properties were set based on the water, and the capillary domain properties were set based on the property of glass. The rounding edge of the capillary was defined to be 4.5 µm based on the microscopic image of the capillary tip (Figure S3). To simulate the "sharp-edge" streaming, the first order field was solved using Thermoviscous Acoustics module. The boundary condition is set by assuming the capillary tip is still and the surrounding fluid is oscillating at **v**_{in}*e^{iωt}. In COMSOL, the left and right vertical walls were given a normal oscillating velocity **v**_{in}. All other boundaries were set as no-slip boundary without any prescribed velocities or pressure. To simulate the bulk vibration of the tip, the first order field was solved using the Acoustic-structure interaction module. In the "Solid Mechanics" module, an xdirection oscillating velocity of vin was given to the whole capillary in the simulation domain. All other boundaries were set as no-slip boundary without any prescribed velocities or pressure. The first order field was simulated in the frequency domain with a set frequency of 94.5 kHz. Multiple frequencies as low as 2.5 kHz and up to 100 kHz were also investigated, and we did not observe change of the streaming patterns. The second order field was simulated as stationary.

For both cases, the F, a source term for streaming originating from the Reynolds stress, can be obtained after solving the acoustic velocity (\mathbf{v}_1) based on eqn (6).

$$F = -\rho \langle (\mathbf{v_1} \cdot \nabla) \mathbf{v_1} \rangle \tag{6}$$

The second order acoustic streaming velocity was then computed using the *Laminar Flow* module of COMSOL with F as the volume force.

Free triangular mesh elements were used in this simulation. The minimum element size and maximum element size were 0.00008 mm and 0.0268 mm, respectively. The maximum element

growth rate was set as 1.1. The convergence was validated by comparing the streaming velocity between the chosen mesh with a reference mesh with 50% more triangles. A difference <2% was considered as acceptable.

Mass Spectrometry (MS) Analysis

A Q-Exactive Hybrid Quadruple Orbitrap mass spectrometer (Thermo Fisher, San Jose, CA, U.S.A.) was used for MS measurements with the epoxy liquid-filled capillary. During the measurements, 1 μ M clarithromycin with 0.01% HCOOH in H₂O was pumped with a flow rate of

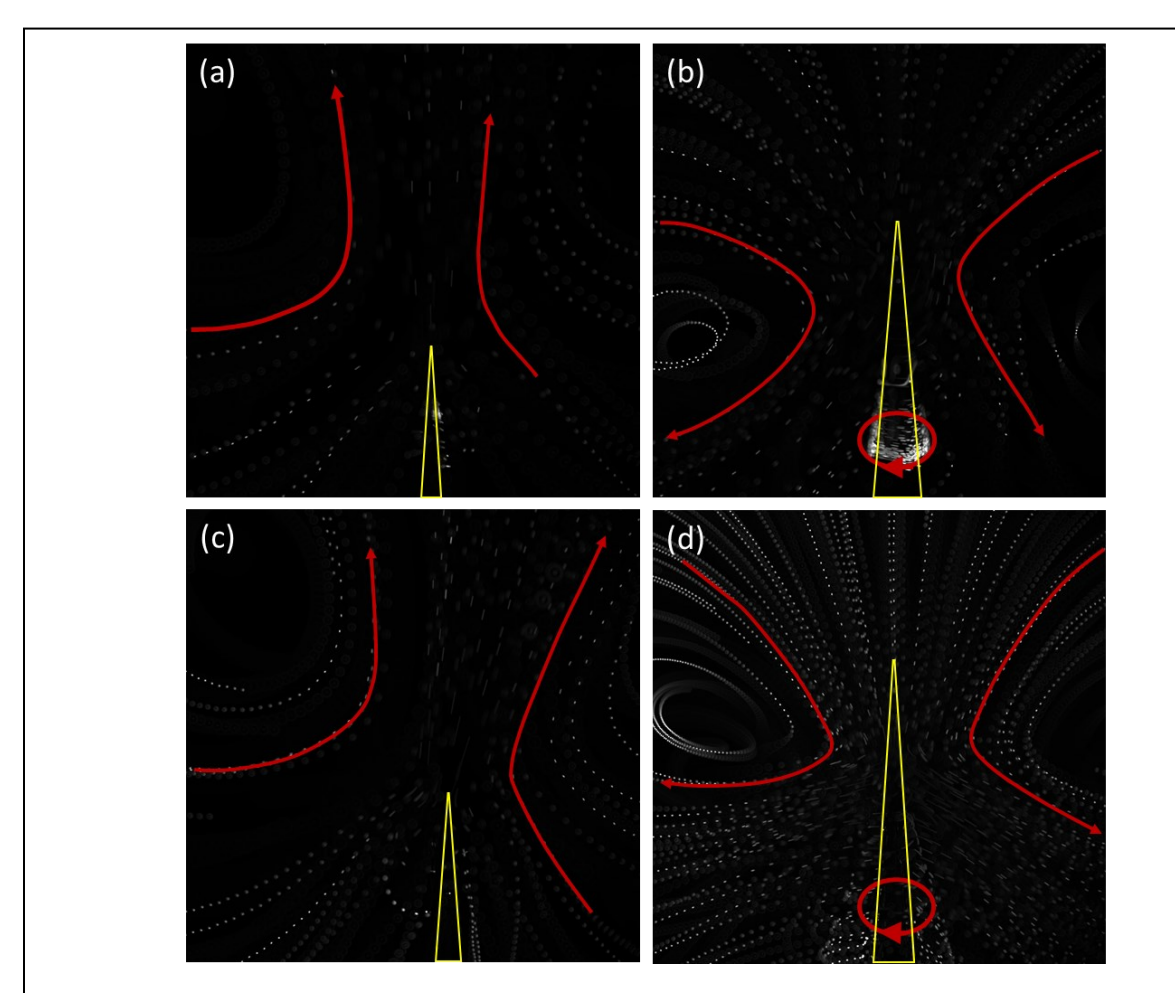


Figure 2. Streaming patterns for the liquid-filled capillary and air-filled capillary. (a) Streaming pattern for the liquid-filled capillary at 94.5 kHz, 2.5 Vpp. (b) Streaming pattern for the air-filled capillary at 94.5 kHz, 8 Vpp. (c) Streaming pattern for the liquid-filled capillary, capillary back end sealed by epoxy glue at 98.5 kHz, 4 Vpp. (d) Streaming pattern for the air-filled capillary, capillary back end sealed by epoxy glue at 94.5 kHz, 7 Vpp.

5 μ L/min (Figure 6). The temperature of the MS inlet capillary was set to 275 °C, and the sheath gas, aux gas, and sweep gas flow rates were all zero. The MS scan type was full MS under positive ion mode, and the mass-to-charge (m/z) range was between 600 – 900. Resolution was

set at 70000 with micro-scans of 2. The MS Automatic Gain Control (AGC) target value was 5e6. The S-lens level was 50. The mass spectrum of clarithromycin was collected under continuous acquisition state for 2 min.

Results and discussion

Patterns of acoustic streaming of a vibrating capillary

To study the acoustic streaming pattern, we immersed the vibrating sharp capillary into a reservoir that was filled with the 10 µm fluorescent bead solution (Figure 1c). The beads will move along with the streaming flow so that the streaming pattern will be visualized. The glass capillary is pulled to a 20 µm I.D. and was placed at the center of the reservoir. The space of the reservoir is large enough so that the wall of reservoir has minimal impact on the streaming flows. The liquidfilled capillary and the air-filled capillary were prepared based on the procedure described in the experimental section, respectively. Since the liquid level also affects the acoustic streaming of a vibrating capillary, we maintained the same amount of solution (1 mL) for all the streaming experiment. We tested streaming patterns for both the liquid-filled capillary and air-filled capillary. The working frequency for each capillary was determined by when the beads had highest velocity between 90 kHz to 100 kHz. The streaming pattern figures were generated by stacking the individual pictures that were taken within 15 s, and the streaming lines were the trajectories of the moving beads (Supporting Video 1&2). As shown in Figure 2a, we saw the beads moving upwards for liquid-filled capillary, and near the glass capillary surface there was no clear bead movements, whereas downwards beads movement was observed for air-filled the capillary (Figure 2b). At around 1000 µm below air-filled capillary tip top end, some beads rotate around the capillary surface in a circular trajectory (Figure 2b, the red circle with arrow represents the rotating beads trajectory). These observations demonstrated that the liquid-filled was a factor that led to the change of streaming pattern for the glass capillary.

The distinct streaming direction between the liquid-filled capillary and air-filled capillary could be related with the pumping effect generated by the vibrating capillary when liquid is present inside the capillary. To determine the impact of the pumping effect, we further modified the capillary to prevent the liquid flow transporting out of the capillary. We used epoxy glue to seal the capillary's back end, which effectively suppressed the fluid flow either in or out of the capillary. The epoxy glued liquid-filled capillary and air-filled capillary still showed similar streaming patterns as the no glue capillaries, respectively (Figure 2a v.s. Figure 2b v.s. Figure 2d). For the epoxy glued liquid-filled capillary, it also showed upwards streaming and the streaming lines were almost

same with the OTS coated liquid-filled capillary (Figure 2a and 2c). The epoxy glued air-filled capillary had downwards streaming, and the left side streaming center was observed, together with beads rotating around the capillary surface (Figure 2d), which were similar with the streaming patterns from OTS coated air-filled capillary (Figure 2b). These results indicate that the pumping effect when liquid is present did not cause the difference in streaming direction between the liquid-filled capillary and air-filled capillary. In addition, we examined how much liquid in the capillary is necessary to cause the change of streaming pattern. For an air-filled capillary, when the liquid plug was less than ~3 mm long from the capillary, the streaming pattern was still the same as the air-filled capillary. When the length of the liquid plug continued to increase above ~3 mm, the streaming pattern changed, and the new pattern followed the liquid-filled capillary. This observation further excluded the contribution of fluid flow to the difference in streaming pattern.

To evaluate the impact of acoustic radiation force on the particle trajectory, we also examined the streaming patterns using 2 µm fluorescent particles. The resulting streaming patterns were similar to the ones shown in Figure 2. The distinct streaming patterns between liquid-filled capillary and air-filled capillary could still be observed, indicating that the unique acoustic streaming phenomenon is not caused by acoustic radiation force. It should be noted that acoustic radiation force may play a role in trapping particles around the vibrating capillary as shown in Figure 2b.

To exclude the impact of reservoir size on the streaming patterns, we fabricated 4 additional sizes of reservoirs (10*10, 15*15, 30*30, and 40*40 mm), and observed streaming patterns with both liquid-filled and air-filled capillaries. All the streaming patterns agreed with what we observed in the 20*20 mm reservoir used above. Based on these results, we can exclude the impact of reservoir on the streaming direction reversal phenomenon.

As shown in Figure 2, the position of the two vortex centers in both streaming patterns was also different. For the liquid filled capillary, the vortex center is further away from the capillary and is ~1500 µm above the capillary (Figure 2a and 2c), whereas the vortex center of the OTS coated air-filled capillary and epoxy glued air-filled capillary are ~ 900 µm (Figure 2b) and 500 µm (Figure 2d) below the capillary top end, respectively. The difference in the position of the vortex centers could be related with the difference in the vibration modes under the two setups. When liquid is present, the vortex centers are above and further away from the tip, indicating that the vibration of the tip contributes mainly to this pattern. When liquid is absent, the vortex centers are below and closer to the capillary tip, and beads rotating around the capillary wall were observed. These observations indicate that the bulk vibration of the capillary is the major contributor to the streaming pattern. Interestingly, the streaming pattern when liquid is present closely resembled

the "sharp-edge" acoustic streaming that is reported by Ovchinnikov et al. (Ovchinnikov, Zhou et al. 2014) In contrast, the air-filled capillary streaming seems to be similar to the streaming generated by the ultrasonic needle, which is originated from the bulk vibration of the solid object. (Tang, Liu et al. 2018)

To confirm this finding, we performed numerical modeling of acoustic streaming under the two assumptions, respectively. The simulation of acoustic streaming is based on the perturbation method, and the detail of the model is provided in the experimental section. We set up two models to simulate the "sharp-edge" streaming and bulk vibration induced streaming, respectively. As shown in Figure 3a, the boundary conditions of the "sharp-edge" streaming simulation are set by giving an oscillating velocity to the two vertical walls of the simulation domain. This boundary condition assumes that a vibrating tip in the quiescent liquid is equivalent to a still tip in an oscillating fluid. To simulate the bulk vibration of the capillary, an oscillating velocity was applied to the capillary tip directly in the acoustic-structure interaction module in COMSOL (Figure 3c). Based on the above-mentioned boundary conditions, acoustic streaming patterns were simulated for "sharp-edge" streaming and capillary vibration, respectively (Figure 3b and 3d).

Figure 3b showed that the simulated streaming pattern matches the streaming pattern generated by the liquid-filled capillary. The simulated outwards streaming direction was same with experimental streaming direction, and the simulated two vortex centers were above the capillary end, which was in accordance with the observed vortex (Figure 2a and 2c). Figure 3d showed that the simulated streaming pattern matches the streaming pattern generated by the air-filled capillary (Figure 3b and 3d). Unlike the simulation results for liquid-filled capillary, the streaming direction of air-filled capillary was inwards, and the vortex centers were closer to the capillary end. The difference of the second order acoustic streaming must originate from the difference in the first order field. In Figure S4, we plotted the first order flow, which shows that the air-filled tip showed higher vorticity of the first order velocity field compared with the liquid filled tip. The different boundary conditions (prescribing a periodic velocity perpendicular to the capillary vs. prescribing a vibration velocity to the capillary) give different first order flow structures, which leads to different second order streaming directions.

Based on the simulation results, when the boundary condition was defined according to the sharpedge streaming simulation, the resulting streaming pattern agreed with the liquid filled capillary experimental observation. When the boundary condition was set based on the vibration of the whole capillary, the resulted streaming pattern agreed with the air-filled capillary case. Although the simulation does not elucidate the mechanism of the influence of liquid on acoustic streaming, it indicates the different origins of the two observed streaming patterns. For the liquid filled tip, the resulting streaming pattern mainly originates from the vibrating tip region, whereas the contribution from capillary wall vibration cannot be neglected for the air-filled tip. This difference could be caused by the presence of liquid (water) affecting the mechanical property of the capillary. The presence of liquid limits the vibration of the bulk capillary, leading to sharp-edge like streaming pattern. When the liquid is absent, the capillary end experience more of the bulk vibration amplitude, leading to vibrating wall induced streaming patterns.

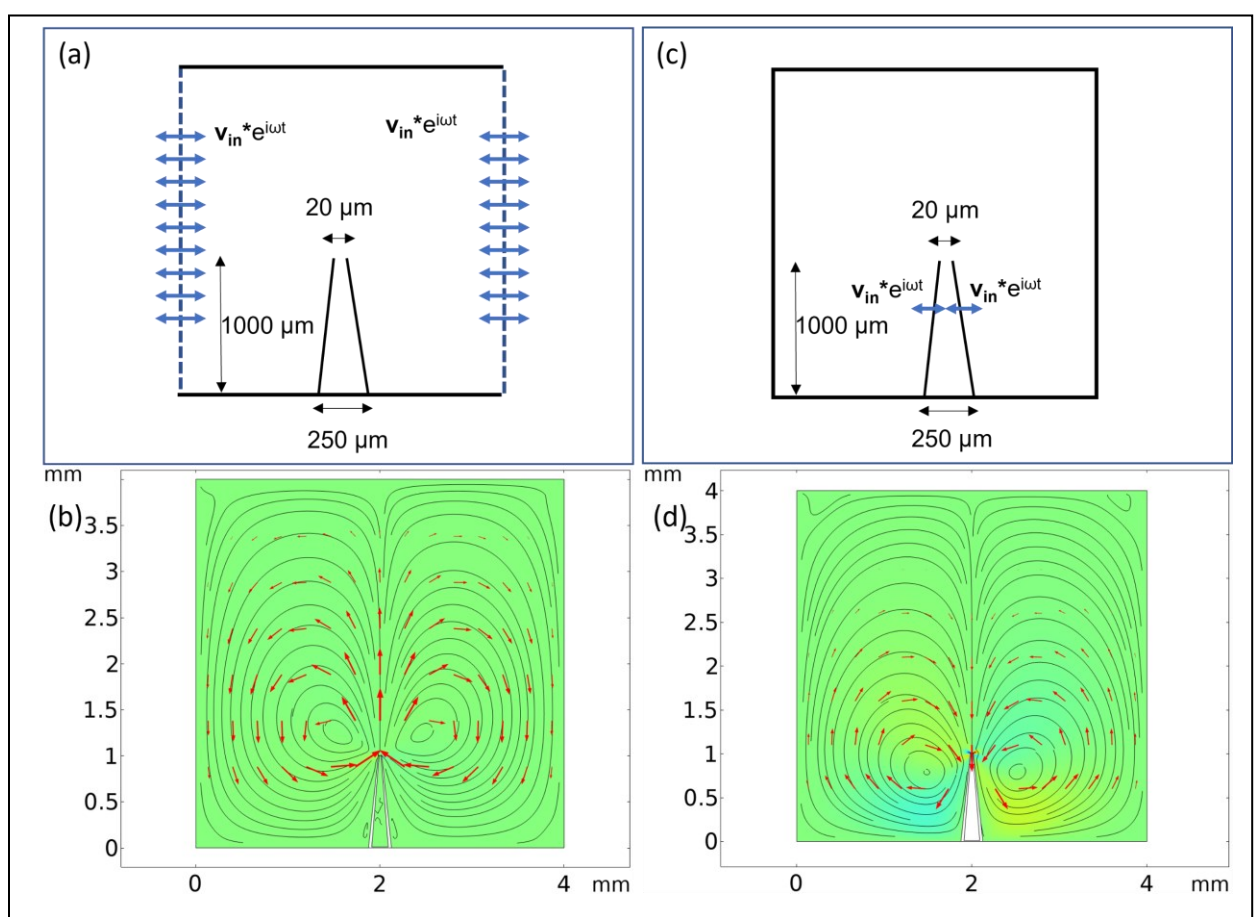


Figure 3. COMSOL simulation for the liquid-filled capillary and air-filled capillary streaming patterns. (a) General geometry, length scales and boundary conditions of the liquid-filled capillary. (b) Simulated streaming pattern for the liquid-filled capillary. (c) General geometry, length scales and boundary conditions of the air-filled capillary. (d) Simulated streaming pattern for the air-filled capillary. Red arrows represent the simulated streaming directions.

Streaming Velocity

Next, we examined the practical consequence of the two capillary setups. In addition to the streaming pattern, another notable difference between liquid-filled capillary induced streaming and air-filled capillary induced streaming was the streaming velocity. For the liquid filled capillary,

the streaming velocity is significantly higher than the air-filled capillary under the same input amplitude. To examine this difference quantitatively, we measured the streaming velocity under different input amplitudes for the liquid-filled capillary and air-filled capillary, respectively. We used 10 µm beads to visualize the streaming line and the movement velocity of the beads should reflect the velocity of acoustic streaming. The beads velocity was measured based on the moving distance of the bead between two picture frames and divided by the time interval between these two adjacent picture frames. Since the beads velocity is not uniform as it circles around the vortex center, we chose the beads in the fastest velocity area and to calculate the bead moving velocity. The working amplitude range we chose was from 5 Vpp to 10 Vpp. Below 5 Vpp, the 10 µm beads moved slowly and the bead moving distance between two adjacent frames was too small and difficult to measure; Above 10 Vpp, the bead moving velocity was too high to capture, which is limited by the field of view and image acquisition rate of the microscope. As shown in Figure 4a, between 5 Vpp to 10 Vpp, all the streaming velocities of epoxy glued liquid-filled capillary were higher than the air-filled capillary. When the amplitude went higher, the streaming velocity of the liquid-filled capillary increased sharply, whereas the increase for air-filled capillary was not obvious. At 5 Vpp, both the epoxy glued liquid-filled capillary and air-filled capillary had a low velocity, which were 15 mm/s and 2.7 mm/s, respectively. However, when the input power was increased to 10 Vpp, the streaming velocity for liquid-filled capillary was above 100 mm/s, but the streaming velocity of air-filled capillary was only around 10 mm/s. We also measured the streaming velocity for the OTS coated capillary, and we observed a similar velocity trend and streaming velocities for both the OTS coated liquid-filled and air-filled capillary (Figure 4b). At 5 Vpp, the streaming velocity of OTS coated liquid-filled and air-filled capillary were 20 mm/s and 4 mm/s, respectively. With the input power increase, both the streaming velocities for OTS coated liquid-filled and air-filled capillary went up gradually. At 10 Vpp, the streaming velocity of the OTS coated liquid-filled capillary was 75 mm/s, whereas the OTS air-filled capillary was only 16 mm/s. These results suggest that compared with air-filled capillary, the liquid-filled capillary has higher streaming velocity, and with the increase of input amplitude, the streaming velocity enhancement for liquid-filled capillary is more significant than the air-filled capillary. Based on the perturbation theory, the streaming velocity is expected to be proportional to the square of input voltage. We examined our results for this relationship by plotting Vpp² vs. streaming velocity for all the four groups measured here. As shown in Figure S5, good linearity was achieved in all 4 cases with R² ranging from 0.9394-0.9950. The only exception is for the epoxy glued liquid-filled tip, where we have to remove the first two data points for good linearity.

Enhanced mixing performance with liquid-filled capillary

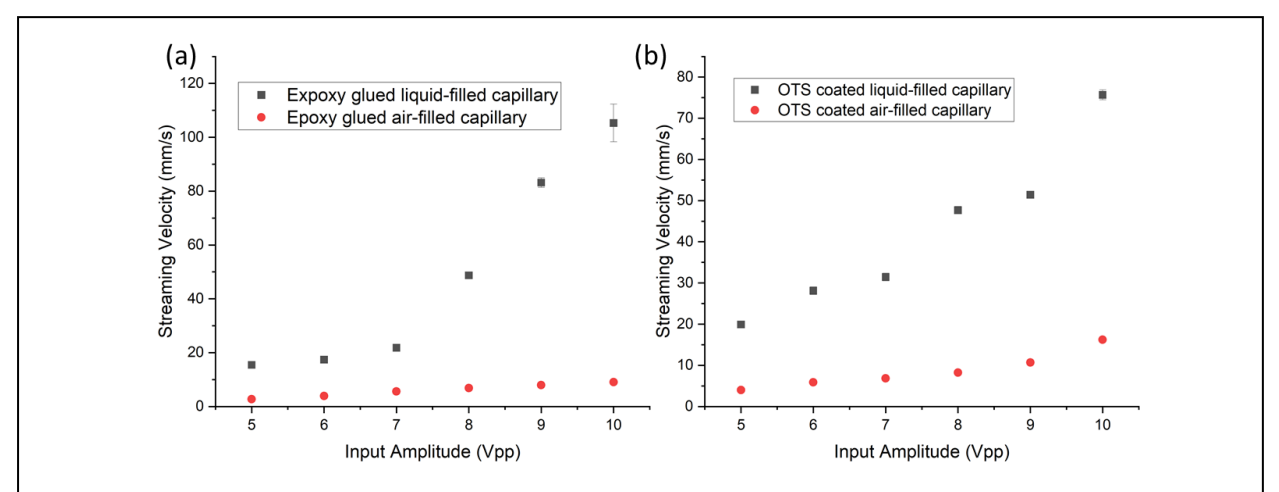


Figure 4. Streaming velocity measurement for liquid-filled capillary and air-filled capillary. (a) Streaming velocity for epoxy glued liquid-filled capillary and epoxy glued air-filled capillary. (b) Streaming velocity for OTS coated liquid-filled capillary and OTS coated air-filled capillary.

Under the same input amplitude, liquid filled capillary showed much higher streaming velocity that the air-filled capillary, which can be further leveraged to improve the energy efficiency of acoustic mixer. Acoustic mixing is achieved through the chaotic streamlines generated by the dissipation of acoustic energy. With the increase in streaming velocity, we examined if this can be translated into improved mixing performance. The higher streaming velocity generated by the liquid-filled capillary was expected to facilitate the rapid mixing. For comparison, we set up the epoxy glued liquid-filled capillary and epoxy glued air-filled capillary into a reservoir, with 1 mL water added into the reservoir. To visualize the mixing process, we added one drop (5 µL) of KMnO₄ solution (1.2 mg/mL) into the reservoir center to compare the mixing speed of the liquid-filled capillary and air-filled capillary (Figure 5a and 5b). Initially, the KMnO₄ solution has a dark-red color (Figure 5a and 5b, 0 s). With time elapse, the liquid-filled capillary can quickly disperse the dark red color KMnO₄ into the reservoir and the color changes within 1.5 s shows the KMnO₄ moves along with the upwards streaming direction that generated by the liquid-filled capillary (Figure 5a, 0.5 s - 1.5s). At 2 s, the KMnO₄ was mixed into the area which was covered by the streaming vortex of liquidfilled capillary (Figure 5a, 2 s, the reservoir area above the capillary top end). However, for the air-filled capillary (Figure 5b), from 0.5 s to 2 s, most of the KMnO₄ still aggregated at the area which was close with the capillary top end or below the capillary top end, and the color patterns of KMnO₄ from air-filled capillary agreed with the streaming pattern that observed for the air-filled capillary in Figure 2b and 2d. The visualized 2 s - mixing process for both liquid-filled capillary and air-filled capillary also match with the streaming phenomena that we observed for liquid-filled and air-filled capillary. Owing to the higher streaming velocity from the liquid-filled capillary, higher mixing performance for KMnO₄ with water was obtained.

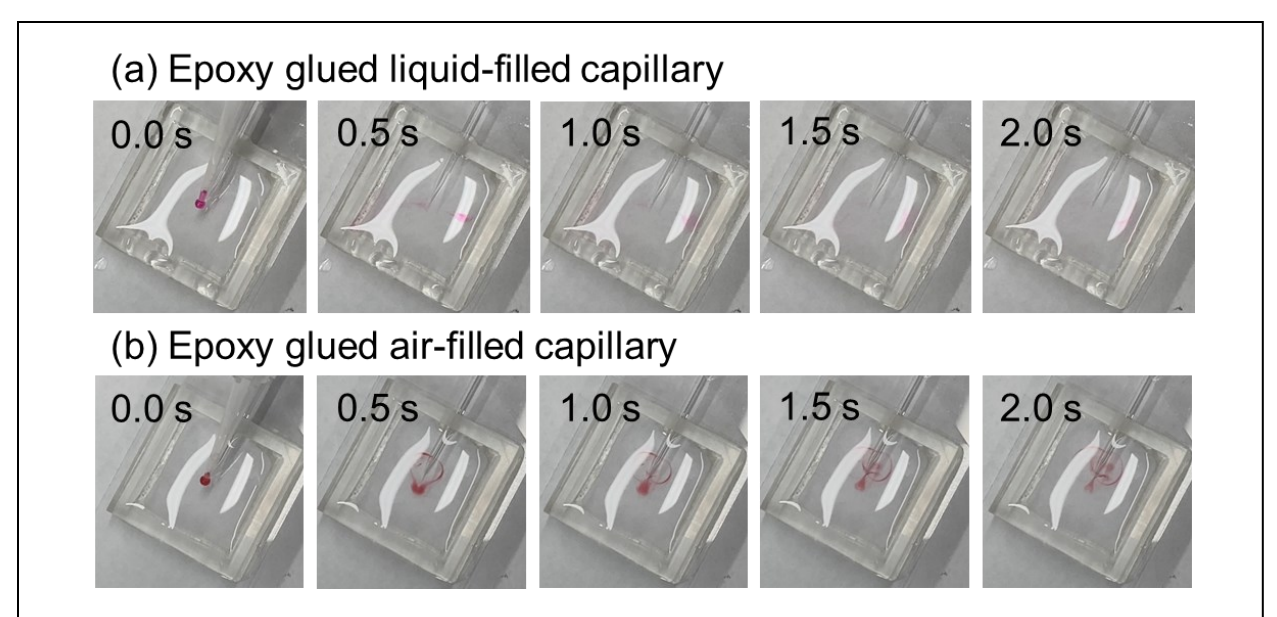
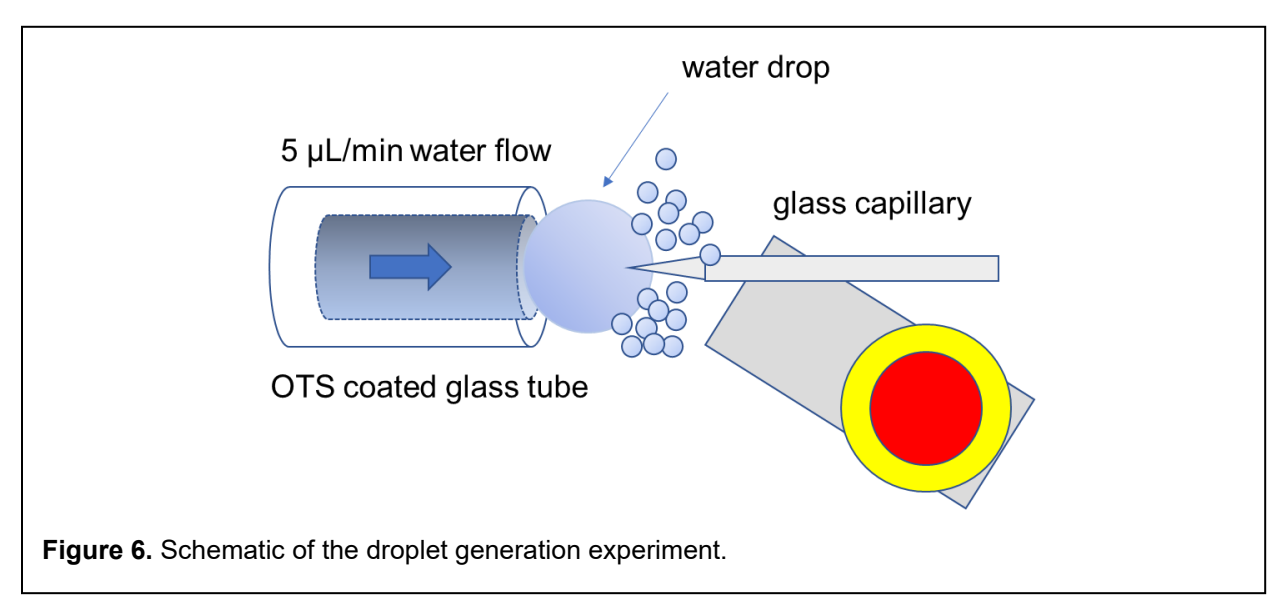


Figure 5. 2 s rapid mixing with epoxy glued capillary. (a) Mixing from 0 s - 2 s with the epoxy glued liquid-filled capillary. (b) Mixing from 0 s - 2 s with the epoxy glued air-filled capillary. $5 \mu \text{L}$ of KMnO₄ in water was dropped into the reservoir center. Device working parameter: 94.5 kHz, 5 Vpp.

Enhanced droplet generation performance with liquid-filled capillary



Another important application for the vibrating capillary is to generate fine liquid droplets in the air for mass spectrometry (MS) analysis. It has been used as an efficient tool for coupling CE with MS analysis. (Kristoff, Li et al. 2020) Here, we examined whether the increase in streaming velocity will also facilitate the droplet generation in a vibrating capillary and MS setup. The schematic of droplet generation with sharp tip capillary is shown in Figure 6. A pump was used to provide a continuous water flow of $5 \,\mu$ L/min, and the water will come out from a glass tube (4 mm

I.D.) coated with OTS. Because the wall surface of glass tube was hydrophobic, a water drop will grow at the outlet of glass tube and finally touch the vibrating glass capillary. For the epoxy glued liquid-filled capillary, once the capillary was touched with the liquid, smaller water droplets were generated immediately. And the video analysis by ImageJ software showed the droplets generation happened within 59 ms (Figure 7a, at 59 ms) for the epoxy glued liquid-filled capillary. The droplet generation will consume the water from the large water drop, and the large water drop shrank its size and no longer touched the vibrating capillary (Figure 7a, 118 ms). With the continuous flow from glass tube, the water drop will grow, touch the vibrating liquid-filled glass capillary, then droplet generation will occur, and the second time for droplet generation with epoxy glued capillary happened at 767 ms (Figure 7a, 767 ms). The droplet generation process will repeat with a time interval of 708 ms for the epoxy glued liquid-filled capillary. However, for the epoxy glued air-filled capillary, no droplets were generated under the same working amplitude. The large water drop grew along the air-filled capillary from 0 ms to 826 ms (Figure 7b), and at the same time this large water drops kept oscillating. These results showed that the liquid-filled capillary can also improve the energy efficiency of the droplet generation.

With the droplet generation from epoxy glued liquid-filled capillary, we moved the droplet generation set-up in front of mass spectrometer to analyze a clarithromycin sample. A clean spectrum of clarithromycin was obtained, and the spectrum was dominated by the protonated clarithromycin ions (Figure 7c, [M+H]⁺, *m/z* 748.48). The average ion intensity level was at 1.45 × 10⁵. In contrast, the epoxy glued air-filled capillary did not generate any MS spectra with the same droplet generation set-up due to the lack of droplet generation.

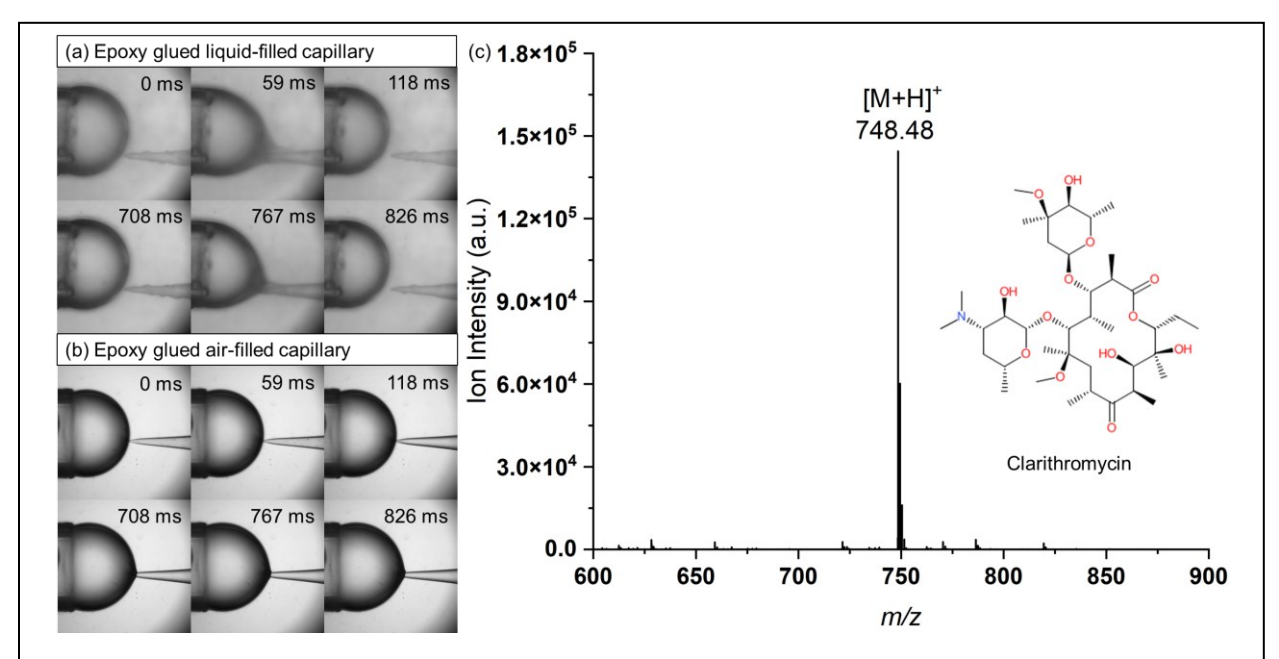


Figure 7. Droplets generation experiments with liquid-filled and air-filled capillary. (a) Droplet generation with the epoxy glued liquid-filled capillary. Device working parameter: 94.3 kHz, 12 Vpp. (b) Droplet generation with the epoxy glued air-filled capillary. Device working parameter: 94.8 kHz, 12 Vpp. (c) Mass spectrum of 1 μ M clarithromycin with 0.01% HCOOH in H₂O. Mass spectrum was obtained with epoxy glued liquid-filled capillary. Device working parameter: 94.5 kHz, 18 Vpp.

Conclusion

In this work, we studied the impact of liquid inside the vibrating glass capillary on its streaming patterns. Our results show that the liquid inside the glass capillary can change the streaming patterns of vibrating glass capillary as well as enhance the streaming velocity under the sample power input. The higher streaming velocity generated by liquid-filled capillary will improved the performance of the vibrating capillary for liquid mixing and droplet generation applications. With the improved droplet generation efficiency, the liquid-filled capillary is expected to improve the performance for CE-VSSI-MS analysis. The present report a simple strategy to improve the energy efficiency of vibrating capillary for generating acoustic streaming. For future studies, systematic optimization of the capillary tip geometry can be combined with the liquid presence to further improve the performance vibrating capillary for various applications.

Acknowledgements

This work is supported by National Science Foundation (CHE-2004021).

References.

Açıkalın T, Raman A, Garimella SV (2003) Two-dimensional streaming flows induced by resonating, thin beams. The Journal of the Acoustical Society of America 114:1785. https://doi.org/10.1121/1.1610453

Ahmed D, Mao X, Shi J, et al (2009) A millisecond micromixer via single-bubble-based acoustic streaming. Lab Chip 9:2738–2741. https://doi.org/10.1039/B903687C

Bachman H, Huang P-H, Zhao S, et al (2018) Acoustofluidic devices controlled by cell phones. Lab Chip 18:433–441. https://doi.org/10.1039/c7lc01222e

Bruus H, Dual J, Hawkes J, et al (2011) Forthcoming Lab on a Chip tutorial series on acoustofluidics: Acoustofluidics—exploiting ultrasonic standing wave forces and acoustic streaming in microfluidic systems for cell and particle manipulation. Lab Chip 11:3579–3580. https://doi.org/10.1039/C1LC90058G

Cardoso VF, Knoll T, Velten T, et al (2013) Polymer-based acoustic streaming for improving mixing and reaction times in microfluidic applications. RSC Adv 4:4292–4300. https://doi.org/10.1039/C3RA46420B

Charrier-Mojtabi MC, Jacob X, Dochy T, Mojtabi A (2019) Species separation of a binary mixture under acoustic streaming. Eur Phys J E Soft Matter 42:64. https://doi.org/10.1140/epje/i2019-11824-9

Costalonga M, Brunet, P, Peerhossaini, H (2015) Low frequency vibration induced streaming in a Hele-Shaw cell, Phys. Fluids 27:013101.

DeBastiani A, Majuta SN, Sharif D, et al (2021) Characterizing Multidevice Capillary Vibrating Sharp-Edge Spray Ionization for In-Droplet Hydrogen/Deuterium Exchange to Enhance Compound Identification. ACS Omega 6:18370–18382.

https://doi.org/10.1021/acsomega.1c02362

Destgeer G, Im S, Hang Ha B, et al (2014) Adjustable, rapidly switching microfluidic gradient generation using focused travelling surface acoustic waves. Appl Phys Lett 104:023506. https://doi.org/10.1063/1.4862322

Du XY, Swanwick ME, Fu YQ, et al (2009) Surface acoustic wave induced streaming and pumping in 128° Y-cut LiNbO3 for microfluidic applications. J Micromech Microeng 19:035016. https://doi.org/10.1088/0960-1317/19/3/035016

Durrer J, Agrawal P, Ozgul A, Neuhauss SCF, Nama N, and Ahmed D (2022)A robot-assisted acoustofluidic end effector. Nat Commun 13: 6370.

He Z, Wang J, Fike BJ, et al (2021) A portable droplet generation system for ultra-wide dynamic range digital PCR based on a vibrating sharp-tip capillary. Biosensors and Bioelectronics 191:113458. https://doi.org/10.1016/j.bios.2021.113458

Huang P-H, Chan CY, Li P, et al (2018) A sharp-edge-based acoustofluidic chemical signal generator. Lab Chip 18:1411–1421. https://doi.org/10.1039/C8LC00193F

Huang P-H, Xie Y, Ahmed D, et al (2013) An acoustofluidic micromixer based on oscillating sidewall sharp-edges. Lab Chip 13:3847. https://doi.org/10.1039/c3lc50568e

Jalal J, Leong TSH (2018) Microstreaming and Its Role in Applications: A Mini-Review. Fluids 3:93. https://doi.org/10.3390/fluids3040093

Kolesnik K, Hashemzadeh P, Peng D, et al (2021) Periodic Rayleigh streaming vortices and Eckart flow arising from traveling-wave-based diffractive acoustic fields. Phys Rev E 104:045104. https://doi.org/10.1103/PhysRevE.104.045104

Kristoff CJ, Li C, Li P, Holland LA (2020) Low Flow Voltage Free Interface for Capillary Electrophoresis and Mass Spectrometry Driven by Vibrating Sharp-Edge Spray Ionization. Anal Chem 92:3006–3013. https://doi.org/10.1021/acs.analchem.9b03994

Li C, Attanayake K, Valentine SJ, Li P (2020) Facile Improvement of Negative Ion Mode Electrospray Ionization Using Capillary Vibrating Sharp-Edge Spray Ionization. Anal Chem 92:2492–2502. https://doi.org/10.1021/acs.analchem.9b03983

Li J, Crivoi A, Peng X, et al (2021a) Three dimensional acoustic tweezers with vortex streaming. Commun Phys 4:1–8. https://doi.org/10.1038/s42005-021-00617-0

Li X, He Z, Li C, Li P (2021b) One-step enzyme kinetics measurement in 3D printed microfluidics devices based on a high-performance single vibrating sharp-tip mixer. Analytica Chimica Acta 1172:338677. https://doi.org/10.1016/j.aca.2021.338677

Li X, Huffman J, Ranganathan N, et al (2019) Acoustofluidic enzyme-linked immunosorbent assay (ELISA) platform enabled by coupled acoustic streaming. Analytica Chimica Acta 1079:129–138. https://doi.org/10.1016/j.aca.2019.05.073

Liang J, Chen K, Xia Y, et al (2020) A localized surface acoustic wave applied spatiotemporally controllable chemical gradient generator. Biomicrofluidics 14:024106. https://doi.org/10.1063/5.0002111

Lin Q, Cai F, Lei J, et al (2021) Numerical study of enhanced Rayleigh streaming in resonant cylindrical shells. J Micromech Microeng 31:104005. https://doi.org/10.1088/1361-6439/ac1ef0

Luong T-D, Phan V-N, Nguyen N-T (2011) High-throughput micromixers based on acoustic streaming induced by surface acoustic wave. Microfluid Nanofluid 10:619–625. https://doi.org/10.1007/s10404-010-0694-0

Majuta SN, DeBastiani A, Li P, Valentine SJ (2021) Combining Field-Enabled Capillary Vibrating Sharp-Edge Spray Ionization with Microflow Liquid Chromatography and Mass Spectrometry to Enhance 'Omics Analyses. J Am Soc Mass Spectrom 32:473–485. https://doi.org/10.1021/jasms.0c00376

Mitome H (1998) The mechanism of generation of acoustic streaming. Electronics and Communications in Japan (Part III: Fundamental Electronic Science) 81:1–8. https://doi.org/10.1002/(SICI)1520-6440(199810)81:10<1::AID-ECJC1>3.0.CO;2-9

Nyborg WBL (1958) Acoustic Streaming near a Boundary, J Acoust Soc Am 30: 329–339

Ovchinnikov M, Zhou J, Yalamanchili S (2014) Acoustic streaming of a sharp edge. The Journal of the Acoustical Society of America 136:22–29. https://doi.org/10.1121/1.4881919

Patel MV, Nanayakkara IA, Simon MG, Lee AP (2014) Cavity-induced microstreaming for simultaneous on-chip pumping and size-based separation of cells and particles. Lab Chip 14:3860–3872. https://doi.org/10.1039/C4LC00447G

Pavlic, A, Harshbarger, CL, Rosenthaler, L, Snedeker, JG, Dual, J (2023) Sharp-Edge-Based Acoustofluidic Chip Capable of Programmable Pumping, Mixing, Cell Focusing, and Trapping. Phys. Fluids 35:022006.

Pavlic, A, Roth, L, Harshbarger, CL, Dual, J (2023) Efficient modeling of sharp-edge acoustofluidics. Frontiers in Physics, 11, 305.

Ranganathan N, Li C, Suder T, et al (2019) Capillary Vibrating Sharp-Edge Spray Ionization (cVSSI) for Voltage-Free Liquid Chromatography-Mass Spectrometry. J Am Soc Mass Spectrom 30:824–831. https://doi.org/10.1007/s13361-019-02147-0

Tang Q, Hu J, Qian S, Zhang X (2017) Eckart acoustic streaming in a heptagonal chamber by multiple acoustic transducers. Microfluid Nanofluid 21:28. https://doi.org/10.1007/s10404-017-1871-1

Tang Q, Liu P, Hu J (2018) Analyses of acoustofluidic field in ultrasonic needle–liquid–substrate system for micro-/nanoscale material concentration. Microfluid Nanofluid 22:46. https://doi.org/10.1007/s10404-018-2064-2

Wang Z, Huang P-H, Chen C, et al (2019) Cell lysis via acoustically oscillating sharp edges. Lab Chip 19:4021–4032. https://doi.org/10.1039/C9LC00498J

Yeo LY, Friend JR (2009) Ultrafast microfluidics using surface acoustic waves. Biomicrofluidics 3:12002. https://doi.org/10.1063/1.3056040

Zhang C (2020) Acoustic streaming around a sharp edge: fundamentals and mixing applications. These de doctorat, Université Paris Cité

Zhang C, Guo X, Royon L, Brunet P (2020a) Acoustic Streaming Generated by Sharp Edges: The Coupled Influences of Liquid Viscosity and Acoustic Frequency. Micromachines 11:607. https://doi.org/10.3390/mi11060607

Zhang C, Guo X, Royon L, Brunet P (2020b) Unveiling of the mechanisms of acoustic streaming induced by sharp edges. Phys Rev E 102:043110. https://doi.org/10.1103/PhysRevE.102.043110